

# Raman scattering study of microcrystals of perovskite titanates

著者	SAKAI Akira, ANZOU Genki, KIKUCHI Atsushi, SERI Osami
journal or publication title	Ferroelectrics
volume	512
number	1
page range	45-51
year	2017-08-09
URL	<a href="http://hdl.handle.net/10258/00009672">http://hdl.handle.net/10258/00009672</a>

doi: info:doi:10.1080/00150193.2017.1355159

# Raman Scattering Study of Microcrystals of Perovskite Titanates

AKIRA SAKAI<sup>1),\*</sup>, GENKI ANZOU<sup>1)</sup>, ATSUSHI KIKUCHI<sup>2)</sup> and OSAMI SERI<sup>2)</sup>

<sup>1)</sup>Department of Information and Electronic Engineering,  
Muroran Institute of Technology, Muroran 050-8585, Japan

<sup>2)</sup>Department of Mechanical, Aerospace, and Materials  
Engineering, Muroran Institute of Technology,  
Muroran 050-8585, Japan

(Received )

Microcrystals of several perovskite titanates ( $\text{ATiO}_3$ , A:Pb, Mn, Ni, Co, Mg) have been synthesized by the corrosion product method. The products were characterized by XRD, SEM, and Micro-Raman scattering. The average size of the microcrystals is estimated to about  $2\mu\text{m}$  by the scanning electron microscope. Micro-Raman scattering spectra show the typical line shapes corresponding to the crystal structures of  $\text{ATiO}_3$ . In the trigonal  $\text{MgTiO}_3$ , the intensities of the several Raman modes take the maximum value at  $50^\circ\text{C}$  as temperature increase from room temperature. It is indicated that the peaks are caused by the impurities rather than the structural change.

*Keywords:* corrosion product, perovskite oxide, Raman scattering, microcrystal

\*Corresponding author. E-mail: sakai@mmm.muroran-it.ac.jp

## 1. INTRODUCTION

Perovskite titanates ( $ATiO_3$ ) have been extensively studied for many technical applications. Since perovskite ceramics are fabricated from perovskite powders, the nano-crystalline powders are synthesized by a lot of methods such as a conventional solid state reaction method [1], wet chemical processes [2], hydroxides [3], sol-gel process [4], and so on. New method using a corrosion product has been proposed to synthesize aluminum-oxide powders [5,6]. It is possible to synthesize at low temperature and to obtain the powder samples with the homogeneous composition. Furthermore, the particle size of powders takes the homogeneous distribution [5,6]. In order to get the powders which have the homogeneous composition and size, we have applied the corrosion product method to synthesize the perovskite oxides.

In the present study, the A-site atoms of  $ABO_3$  were substituted by Pb, Mn, Ni, Co and Mg. In this measurement,  $PbTiO_3$  was selected as a standard sample. Except for  $PbTiO_3$ , above titanates belong to the trigonal ilmenite structure at room temperature.  $MnTiO_3$  undergoes a phase transition from the ilmenite structure to the lithium niobate structure at high pressure 20-30kbar [7].  $NiTiO_3$  is an n-type semiconducting material [8].  $CoTiO_3$  has been used in a wide variety of applications such as gas sensors [9] and catalysts [10].  $MgTiO_3$  has been employed as ceramic capacitors [11] and resonators [12].

Raman scattering spectra of the powder samples of perovskite

titanates ( $\text{PbTiO}_3$ ,  $\text{NiTiO}_3$ ,  $\text{CoTiO}_3$ ,  $\text{MnTiO}_3$ ,  $\text{MgTiO}_3$ ) have been observed by many researchers [13-18]. Their main targets are temperature dependence, particle-size dependence, concentration dependence of compound, and so on. In the micro-Raman scattering method [19], the incident laser beam is easily focused to the micron size. This fact means that we can get the information in the localized area. For this reason, we have used the micro-Raman scattering method to evaluate the powder samples. When the particle sizes of powders are the same size of the focused laser beam, the spectrum of one micro-crystal are detectable. Therefore, micro-Raman scattering is one of the powerful techniques to study the powder samples.

## 2. EXPERIMENTAL PROCEDURE

The powders of perovskite titanates were synthesized by the corrosion product method. Metal powders (Pb, Mn, Ni, Co, Mg) were dissolved in  $\text{HNO}_3$  solution. Ti powder is also dissolved in the mixed solution of  $\text{H}_2\text{O}_2$  and  $\text{NH}_3$ . After two solutions were mixed, aqueous ammonia is added to the solution. To obtain the solid samples, the solution was dried and the solid state substance was baked at 1000~1200°C.

In order to analyze the crystal phases, X-ray diffraction (XRD) was carried out. The observed peaks were in good agreement with those of the previous reports. For example, Fig.1 shows the XRD pattern of the  $\text{NiTiO}_3$  powder. All diffraction lines are well

defined. As shown in Fig.1, the presence of the extraneous substances is very few. The particle size distribution and particle morphology observation were obtained by an automatic particle measurement apparatus and scanning electron microscope (SEM). Figure 2 shows the SEM image of the  $\text{NiTiO}_3$  powder. The form of particles seems a spherical shape. The average particle size is estimated to about  $2\mu\text{m}$ . These measurements confirms us that powder samples have the homogeneous composition and size.

Raman scattering spectra were observed by using a micro-probed Raman system with a back scattering configuration [19]. The laser beam exited at 532 nm was focused to  $2\mu\text{m}$  in spot size on a sample surface. The scattered light was analyzed by a triple grating monochromator with a charge coupled detector. The temperature of the sample was controlled within 0.1 K.

### 3. RESULTS AND DISCUSSION

#### 3.1 Micro-Raman scattering spectra of tetragonal sample

Figure 3 shows the micro-Raman scattering spectra of  $\text{PbTiO}_3$  microcrystals. The spectra were observed in the polarized condition VV and depolarized condition HV. Two spectra show the almost same line shape as shown in Fig.3. The line shape of  $\text{PbTiO}_3$  powder agrees with that of previous report [13]. This fact indicates that the synthesized powder belongs to the tetragonal structure and the synthesized method is good enough to prepare the titanate powder sample.

### 3.2 Micro-Raman scattering spectra of trigonal samples

Micro-Raman scattering spectra of the trigonal perovskite titanates ( $\text{NiTiO}_3$ ,  $\text{CoTiO}_3$ ,  $\text{MnTiO}_3$ ,  $\text{MgTiO}_3$ ), which form the trigonal ilmenite structure, are shown in Fig.4 at room temperature. All spectra are in good agreement to the previous reports [15-18]. Especially, the micro-Raman spectra of  $\text{NiTiO}_3$ ,  $\text{CoTiO}_3$  and  $\text{MnTiO}_3$  are almost same line shapes since Ni, Co and Mn atoms have the almost same atomic mass. Thus, it is confirms us that the crystal structure and the force between the atoms are also same. In the case of  $\text{MgTiO}_3$ , the observed peaks shift to the high frequency side compared with those of  $\text{NiTiO}_3$ ,  $\text{CoTiO}_3$  and  $\text{MnTiO}_3$ . The atomic mass of Mg is 24.3 and that of Mn is 54.9. In general, the lattice mode including light atoms oscillates fast so that the peak shifts to high frequency side. The spectra in Fig.4 are well explained by the mass difference of the A-site atoms.

### 3.3 Temperature dependence of Raman scattering spectra

In the previous section,  $\text{MgTiO}_3$  sample is pure enough according to the X-ray diffraction and micro-Raman scattering. On the other hand, another  $\text{MgTiO}_3$  samples include the extraneous substances are also obtained under the present synthesise condition. To study the behavior of the extraneous substances in the microcrystal, the temperature dependence of the micro-Raman scattering has been carried out from room temperature to 200°C.

Figure 5 shows the temperature dependence of the micro-Raman scattering spectra of the  $\text{MgTiO}_3$  sample. Compared with the spectrum in Fig.4, the new peaks appear as shown in Fig.5 indicated by arrows. The intensities of these peaks show the unusual temperature dependence, though the peak positions do not change in this temperature range. In the case of the cooling process as shown Fig.6, the intensities of the arrowed peaks return to the original intensities at  $30^\circ\text{C}$ . Figure 7 shows the temperature dependence of the intensity of the peak at  $430\text{ cm}^{-1}$ . As the temperature increases, the intensity takes a maximum value at about  $50^\circ\text{C}$  and decreases rapidly. Between the room temperature and  $200^\circ\text{C}$ , the peaks expect for the arrowed peaks do not show the remarkable change. Thus, it is difficult to consider the phase change. Since the peak positions of the arrowed peaks do not change, the force constant and atomic mass rerated to these modes remain unchanged. After the thermal process the intensities return to the original intensities. For these reasons, the extraneous substances do not move during the thermal process. It is pointed out the possibility that the electronic resonance effect at the impurity site may cause the enhancement of the intensity of the additional mode. Thus, the electronic state of the impurity site is effected by the local strain which is induced by the thermal process. To clear this point, it is necessary to carry out the further study.

## REFERENCES

- [1] Henkes A, Bauer J, Sra A, Johnson R, Cable R and Schaak R: Low-temperature nanoparticle-directed solid-state synthesis of ternary and quaternary transition metal oxides. *Chem. of Materials*, 2006;18:567-571.
- [2] Ahuja S and Kutty T: Nanoparticles of SrTiO<sub>3</sub> prepared by gel to crystallite conversion and their photocatalytic activity in the mineralization of phenol. *J. of Photochemistry and Photobiology A-Chemistry*, 1996; 97:99-107.
- [3] Kutty T and Padmini P: Mechanism of BaTiO<sub>3</sub> Formation through Gel-to-crystallite Conversions). *Materials Chem. and Phys.*, 1995;39:200-208.
- [4] Chandler C, Roger C and Hampdensmith M: Chemical Aspects of Solution Routes to Perovskite-phase Mixed-metal Oxides from Metal-organic Preccursors. *Cemical Reviews*, 1993;93:1205-1241.
- [5] Seri O and Sasaki D: Preparation of Aluminumtriethoxide by Application of Aluminum Corrosion. *Materials Transactions*, 2009; 50:1964-1968.
- [6] Seri O, Tsuji T and Sasaki D: Preparation of MnAl<sub>2</sub>O<sub>4</sub> by Corrosion Synthesis. *J.Jpn.Soc.Powder Powder Metallurgy*, 2014;61:153-157.
- [7] Nancy L, Jaidong K and Charles T: A new phase transition in MnTiO<sub>3</sub>: LiNbO<sub>3</sub>-perovskite structure, *Physics and Chemistry of Minerals*, 1989;16:621-629.
- [8] Salvadorl P, Gutiérrez C and. Goodenough JB: Photoelectrochemical properties of n-type NiTiO<sub>3</sub>. *J. Appl.*



Phys., 1982;53:7007-7013.

[9] Chu XF, Liu XQ, Wang GZ and Meng GY: Preparation and gas-sensing properties of nano-CoTiO<sub>3</sub>. Materials Research Bull., 1999;34:1789-1795.

[10] Kazuyuki T, Yasuo U, Shuji T, Takashi I and Akifumi U: Catalyst preparation procedure probed by EXAFS spectroscopy. 2. Cobalt on titania. J. Am. Chem. Soc., 1984;106:5172-5178.

[11] Bernard J, Houivet D, Fallah JE and Haussonne JM: MgTiO<sub>3</sub> for Cu base metal multilayer ceramic capacitors. J. of the European Ceramic Soc., 2004;24:1877-1881.

[12] Ferreira VM, Azough F, Baptista JL and Freer R: Magnesium titanate microwave dielectric ceramics. Ferroelectrics, 1992;133:127-132.

[13] Burns G and Scott BA: Raman Spectra of Polycrystalline Solids; Application to the PbTi<sub>1-x</sub>Zr<sub>x</sub>O<sub>3</sub> System. Pys.Rev.Lett., 1970;1191-1194.

[14] Ishikawa K, Yoshikawa K and Okada N: Size Effect on the Ferroelectric Phase Transition in PbTiO<sub>3</sub> Ultrafine Particles. Phys.Rev.B37, 1988;5852-5855.

[15] Song ZQ, Wang SB, Yang W, Li M, Wang H and Yan H: Synthesis of Manganese Titanate MnTiO<sub>3</sub> Powders by a Sol-gel-hydrothermal Method. Materials Science and Engineering B, 2004;113:121-124.

[16] Lopes KP, Cavalcante LS, Simões AZ, Varela JA, Longob E and Leite ER: NiTiO<sub>3</sub> Powders Obtained by Polymeric Precursor Method: Synthesis and characterization. Journal of Alloys and Compounds, 2009;468:327-332.

[17] Westin G, Jansson K, Pohl A and Leideborg M: All Alkoxide Sol-Gel Route to CoO-TiO<sub>2</sub> Nano-Powders. J. of Sol-Gel Science and Tech. 2004;31:25-29.

[18] Ferri EAV, Sczancoskia JC, Cavalcantea LS, Paris EC, Espinosab JWM, Figueiredob AT, Pizania PS, Mastelaroc VR, Varela JA and Longob E: Photoluminescence behavior in MgTiO<sub>3</sub> powders with vacancy/distorted clusters and octahedral tilting. Materials Chem. and Phys. 2009;117:192-198.

[19] Sakai A, Mizushima T, Moriyoshi C: Raman scattering Spectra of Quasi-Two-Dimensional Crystallization Water in Cu(HCOO)<sub>2</sub>·4H<sub>2</sub>O Near the Antiferroelectric Phase Transition. Ferroelectrics, 2007;346:168-172.

## Figure Captions

FIGURE 1 XRD pattern of NiTiO<sub>3</sub> powder.

FIGURE 2 SEM image of NiTiO<sub>3</sub> powder.

FIGURE 3 Micro-Raman scattering spectra of PbTiO<sub>3</sub> microcrystals of the tetragonal perovskite structure. The spectra were observed in the polarized condition VV and depolarized condition HV.

FIGURE 4 Micro-Raman scattering spectra of NiTiO<sub>3</sub>, CoTiO<sub>3</sub>, MnTiO<sub>3</sub> and MgTiO<sub>3</sub> microcrystals of the trigonal ilmenite structure at room temperature.

FIGURE 5 Temperature dependence of Micro-Raman scattering spectrum of MgTiO<sub>3</sub> microcrystal in the heating process. The peaks indicated by arrows are caused by the impurities.

FIGURE 6 Temperature dependence of Micro-Raman scattering spectrum of MgTiO<sub>3</sub> microcrystal in the cooling process. The peaks indicated by arrows are caused by the impurities.

FIGURE 7 Temperature dependence of the intensity of the peak at 430 cm<sup>-1</sup>. The closed circles were obtained in the increasing temperature process and the open circles were obtained in the decreasing temperature process.

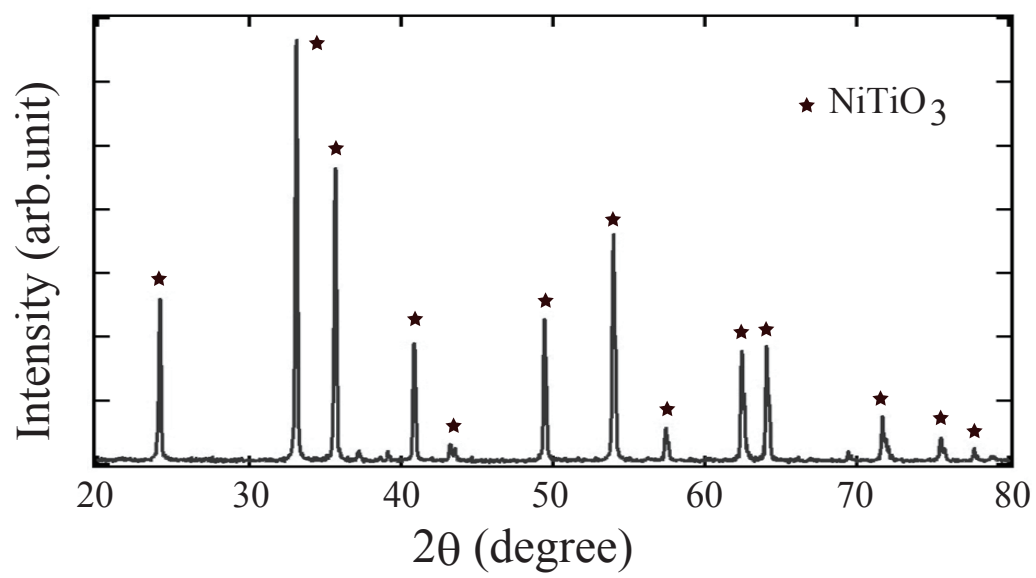


Fig.1

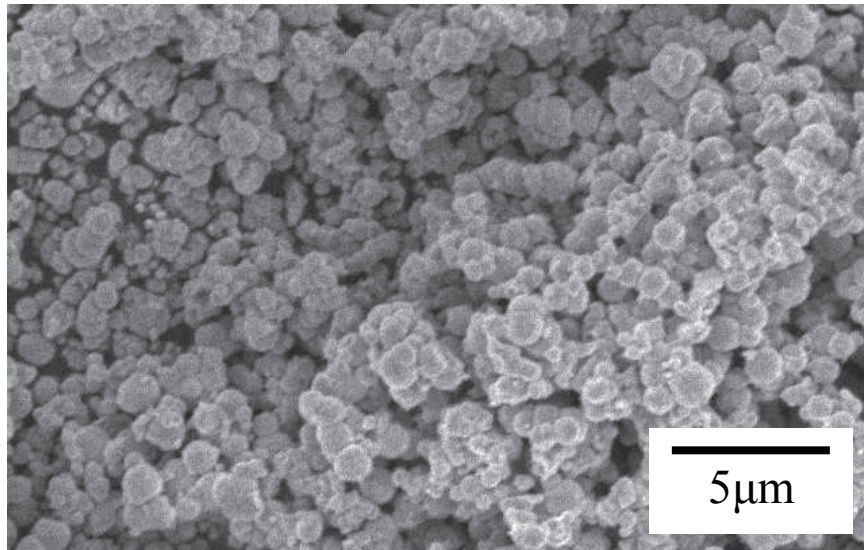


Fig.2

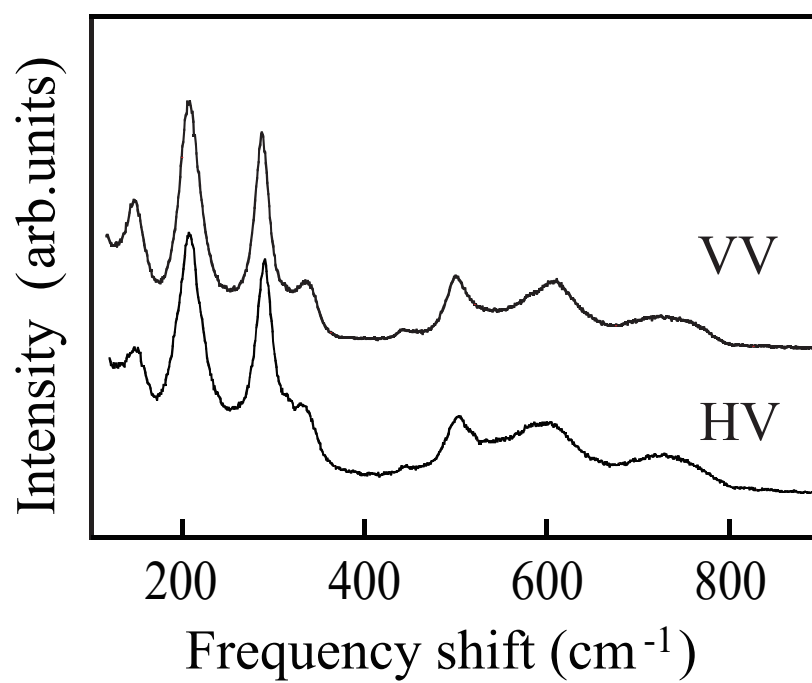


Fig.3

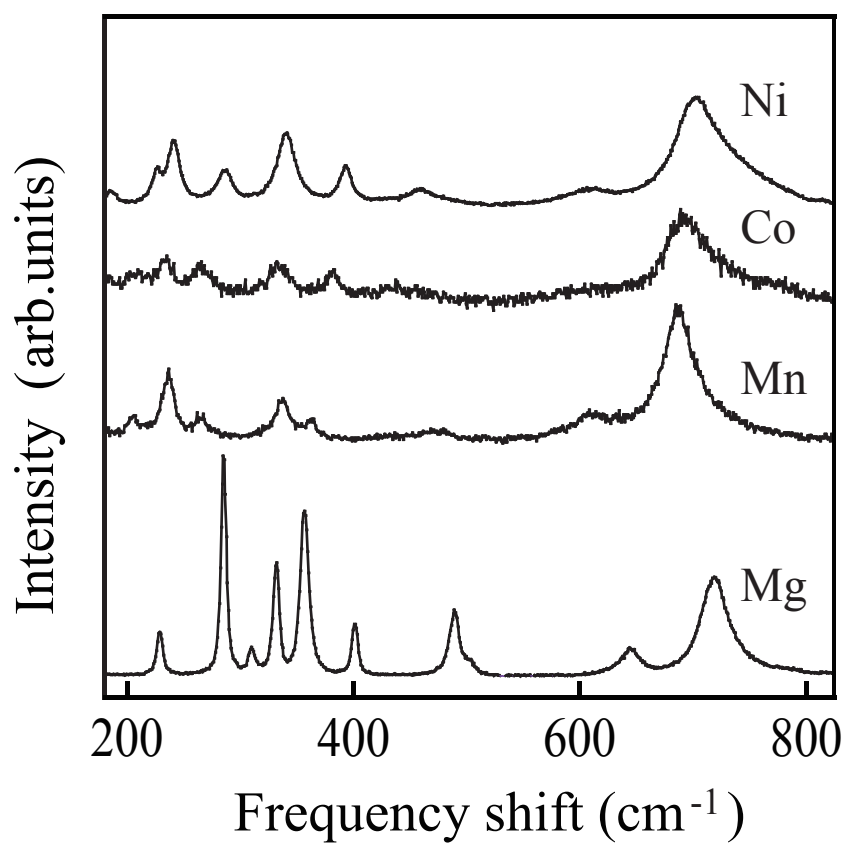


Fig.4

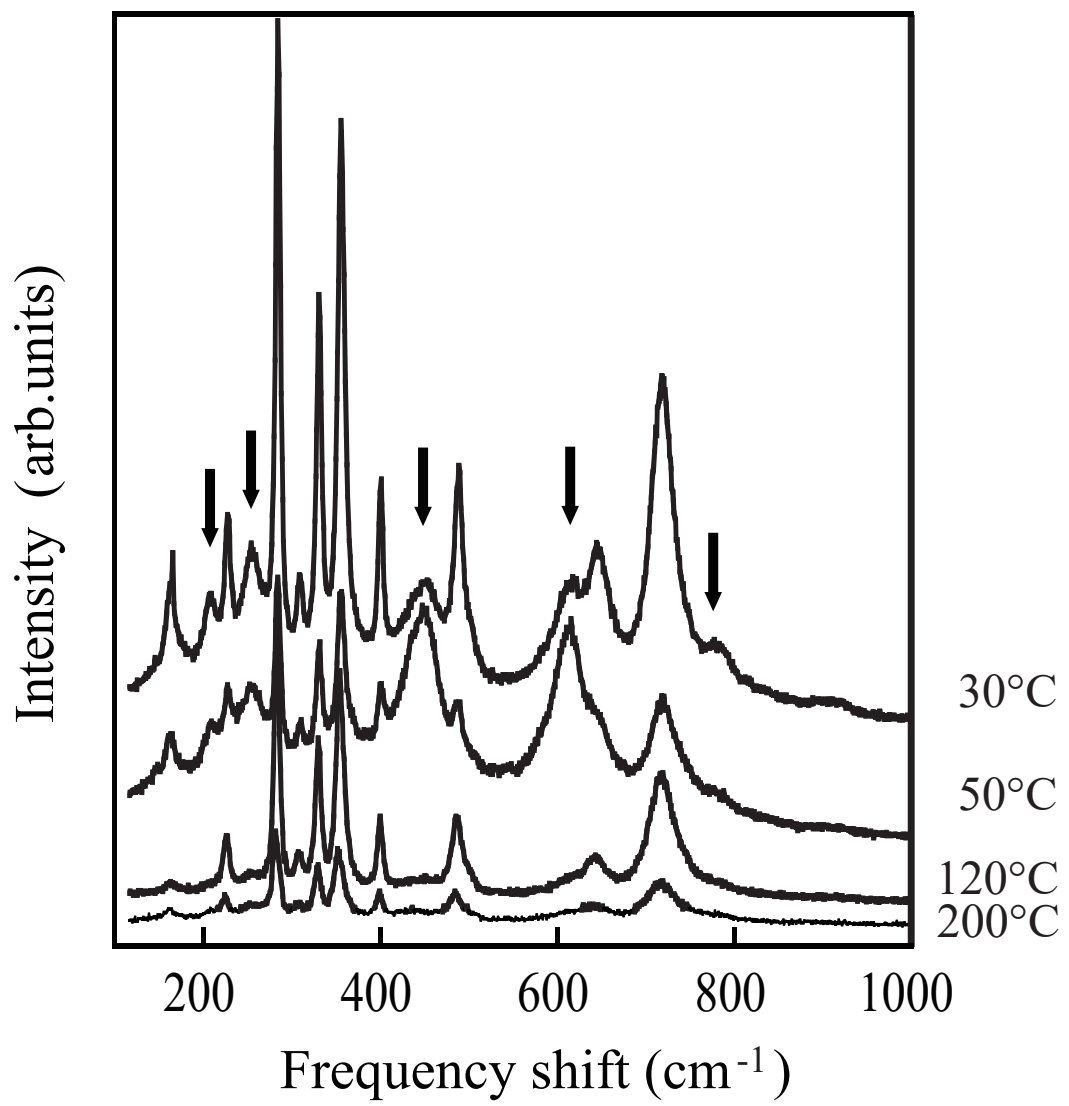


Fig.5



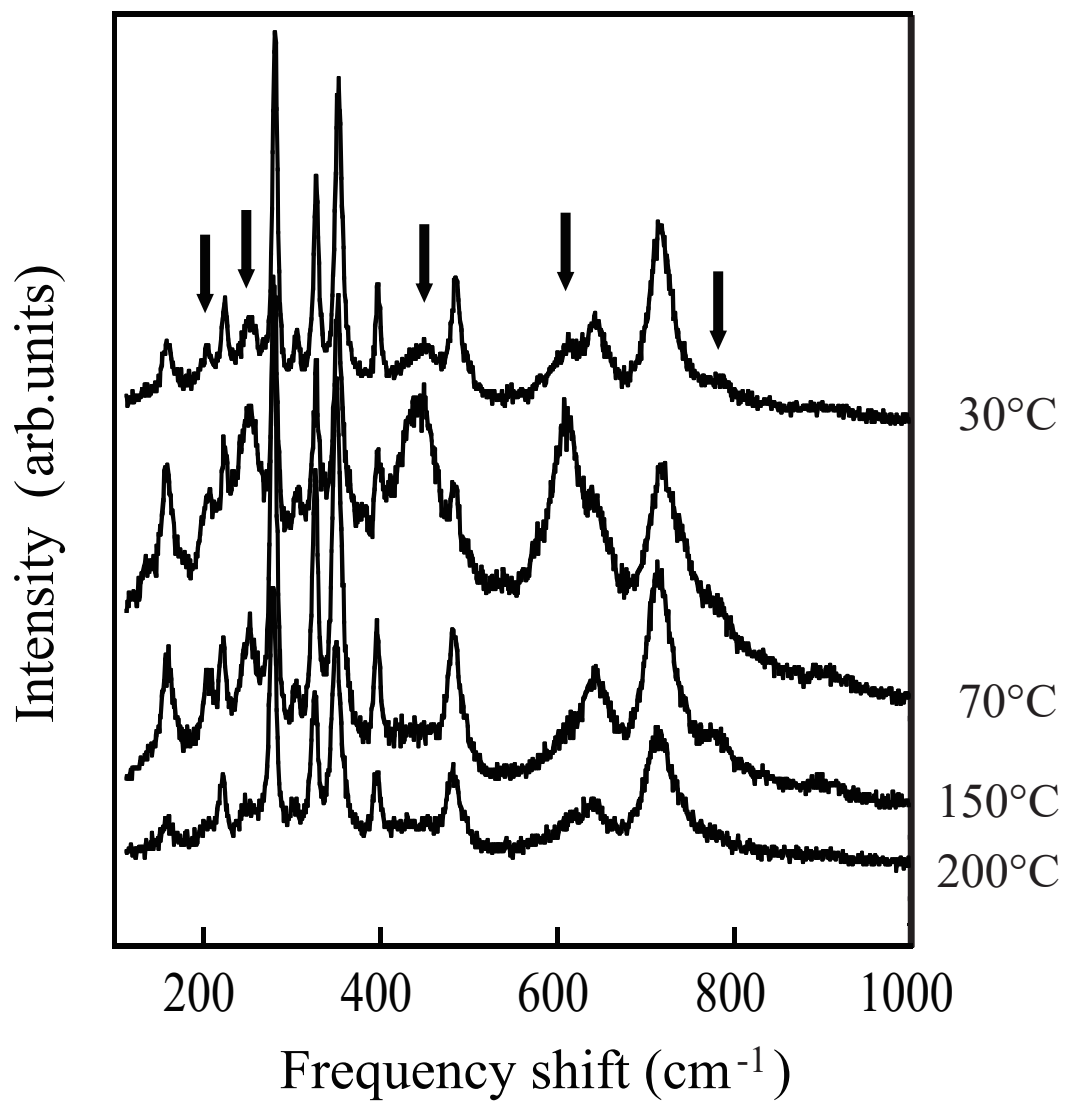


Fig.6

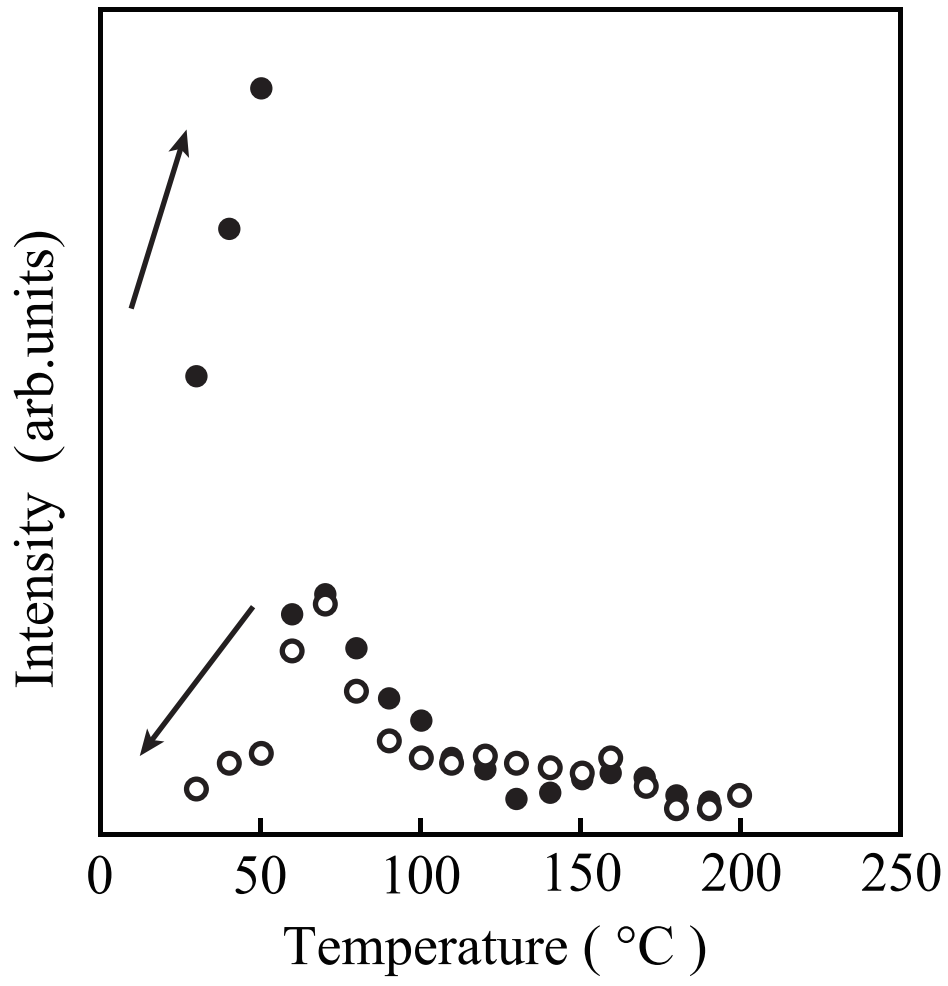


Fig.7